Electrical Engineering in Japan, Vol. 173, No. 2, 2010
Translated from Denki Gakkai Ronbunshi, Vol. 128-B, No. 9, September 2008, pp. 1119–1128

Research on Magnetron Phased Array with Mutual Injection Locking for Space Solar Power Satellite/Station

NAOKI SHINOHARA[1] and HIROSHI MATSUMOTO[2]
[1]Research Institute for Sustainable Humanosphere, Kyoto University, Japan
[2]Kyoto University, Japan

SUMMARY

The SPS (Space Solar Power Satellite/Station) will be a clean base-load power station in space. It will be the largest space system ever built and will require a high-efficiency, large-size, highly accurate, lightweight, inexpensive phased array in order to transmit energy generated in space to the ground. We have proposed and developed a phase-controlled magnetron (PCM) with injection locking and PLL technique for the high-efficiency, lightweight, inexpensive phased array. It still has several weak points: (1) approximately 10% power loss occurs at the circulator for injection locking, (2) phase shifter is needed in each PCM for the phased array. In order to correct the weak points, we propose a magnetron phased array with mutual injection locking. For the magnetron phased array, we only use two PCMs with phase shifters; the other components are self-oscillated and mutual injection locked magnetrons. In this paper, we propose a new formula for use with the magnetron phased array with mutual injection locking. We also present the results of experiments on beam direction control with the magnetron phased array with mutual injection locking. © 2010 Wiley Periodicals, Inc. Electr Eng Jpn, 173(2): 21–32, 2010; Published online in Wiley InterScience (www.interscience.wiley.com). DOI 10.1002/eej.20998

Key words: SPS; magnetron; phased array; injection locking.

1. Introduction

The space solar power satellite/station (SPS) will be a large solar panel satellite in geostationary orbit (36,000 km above the earth) that is beyond the earth's shadow through almost the entire year due to the earth's precession. The electric power generated by it will be sent to the earth by wireless microwave power transmission (electromagnetic waves at 1 to 10 GHz) or laser power transmission. Since the SPS will be 36,000 km above the earth, and the earth's radius is about 6000 km, the SPS will not enter the earth's shadow for most of the year, as shown in the lower left part of Fig. 1 (the diagram represents the summer and winter seasons). Wireless power transmission of microwaves utilizes the so-called "radio window" which is almost free of wave reflection and scattering in the ionosphere, and also of absorption and scattering by the atmosphere or precipitation. As a result, the photovoltaic power can be used even in rainy or cloudy weather. From economic considerations, the usual SPS designed has a usable power above 1 million kilowatts. The SPS is considered a promising energy technology of the future, along with nuclear power plants, which can be operated day and night while emitting hardly any greenhouse gases [1]. Research on microwave wireless power transmission began in the 1960s [2], and the concept of the SPS was first proposed in 1968 [3]. Studies on the base SPS technologies have been

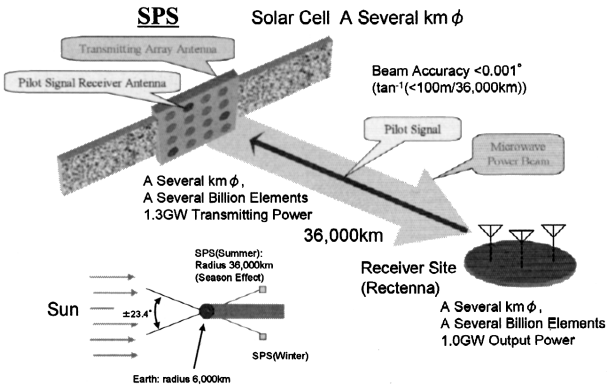

Fig. 1. Concept of SPS.

continuing in the United States since the 1970s [4], and were undertaken in the 1990s in Japan [5–7] and other countries [8, 9]. The energy source of the SPS is in space, and therefore there is a possibility of breaking through the "limits to growth" [10, 11]. According to estimations, the cost of power generation can be reduced to the present level as a result of technological progress [12], thus offering the possibility of commercial power generation in the future.

The SPS must transmit about 1 million kW of electric power over a distance of 36,000 km in order to become a major power source based on clean and economical technologies. This requires solar panels measuring several kilometers on a side, as well as microwave transmitting and receiving antennas of similar size. But the weight of the SPS must be kept to a maximum of 8 to 9 thousand tons. The concept of the SPS is shown schematically in Fig. 1. Research is now under way to solve a number of technological issues, including photovoltaic power generation, collection and distribution of 1 million kW electric power in the space plasma; construction, maintenance, and operation of ultralarge space structures; rocket techniques, etc. The present study deals with microwave wireless power transmission using superlarge array antennas, which is necessary for the implementation of the SPS. Specifically, we propose an easy and inexpensive configuration of phased arrays.

2. Requirements for Microwave Wireless Power Transmission

In microwave wireless power transmission, microwaves themselves are the energy transport medium (carrier). Hence, in contrast to communications and radar technologies, there is no need to impose any information on the carrier (modulation, pulses, etc.). Thus, a nonmodulated continuous wave with a pure spectrum is sufficient, and the frequency band can be narrowed down to the extent allowed by the oscillator's Q-value and the phase noise limit. In addition, in microwave wireless power transmission, one must consider three major losses: the loss of converting electric power into microwaves, the loss related to transmitted microwaves that cannot be collected by the receiving antenna because of spreading, and the loss of reconverting received microwaves into electric power. Researchers aim at 50% efficiency of microwave wireless power transmission (the ratio of the power generated by the SPS in space to the power that can be used on earth). Therefore, the above three losses must be reduced. The receiving end of microwave transmission is usually implemented as a "rectenna," a rectifying antenna with diode. On the other hand, on the sending end, phased array antennas (recently used in radars) must be employed. A phased array is a device composed of multiple antennas with controlled phase and amplitude of the emitted waves. By using wave synthesis, a beam with the desired shape and steerable direction is formed. Therefore, phased arrays do not need mechanical control of the antenna plane, and beam control can be applied to an antenna of arbitrary shape. Since the SPS is a satellite, it is impossible to fix its position and orientation as well as the antenna shape, and therefore the beam must always be controlled so as to point at the receiving site.

At present, applications of phased arrays are restricted to some radars and other devices [13, 14] because these antennas are very expensive by their nature, and precise phase control poses a serious technological challenge. Furthermore, in the case of the SPS, phased arrays must be highly efficient, ultralarge, precise, lightweight, and inexpensive. Existing phased arrays are based on semiconductor amplifiers. In this study, however, we propose and experimentally estimate a magnetron-based phase array featuring very low cost, high accuracy, and an excellent power-to-weight ratio.

3. Phase-Controlled Magnetron and Injection Locking

The magnetron is a microwave oscillator used in microwave cookers. Oscillation by means of an electric field, a magnetic field, and a resonant cavity provides very high efficiency (over 70%) and high output (1 kW and more), and the generation cost is several orders of magnitude cheaper than other microwave sources [about 1000 yen per unit (kW)]. However, a high oscillation output implies difficulty of phase control as well as a low Q-value and strong noise. For these reasons, the use of magnetrons has been restricted to heating appliances such as microwave cookers, and some pulse radars. In this context, we have shown that magnetron noise is related to the stability of the power source and the temperature of the electron emission filament, and that Q-values above 1×10^5 can be achieved even in the self-excited magnetron state if a DC stabilized source is used [15]. We also showed that noise can be kept below –100 dBc on both the low- and high-frequency sides, except for n-th-order harmonics that are inevitably produced because of the magnetron's cylindrical structure. However, the n-th-order harmonics can be kept below –60 dBc, which makes it possible to use the magnetron for applications other than heating. We have shown experimentally that magnetron noise is generated during the rise or fall time of the half-wave voltage doublers used in microwave cookers, or of the pulsed power supplies used in radars [16]. In a DC stabilized power supply maintaining the rated voltage, the spectral Q-value can be increased by more than three orders of magnitude while keeping noise below –100 dBc.

It has been shown that such magnetrons can also be utilized for microwave energy transfer. However, there have been no phase control methods for self-excited magnetrons, and frequency variation with temperature still remains a problem. We therefore developed a phase-controlled magnetron (PCM) that provides phase control of conventional inexpensive magnetrons for microwave cookers by using two phenomena. The first is that the magnetron frequency varies with the applied voltage and current, and the second is that when weak reference microwaves are injected from outside, the magnetron frequency is locked to the frequency of the reference microwaves [17]. The latter phenomenon is called injection locking, and contributes to frequency stability; it was formulated by Adler as follows:

$$\frac{\Delta\omega}{\omega_0} = \frac{2}{Q_{ext}}\sqrt{\frac{P_i}{P_o}} \tag{1}$$

Here ω_0 is the self-oscillation frequency of the magnetron, Q_{ext} is the external Q-value of the magnetron, P_o is the amplitude of the magnetron, P_i is the injected signal amplitude, and $\Delta\omega$ is the injection-lockable frequency range: that is, if the difference in frequency between the magnetron and injected signal is within $\Delta\omega$, then the former frequency can be locked to the latter. Frequency locking is determined by Eq. (1), and the phase shift proportional to $\Delta\omega$ remains as follows:

$$\frac{d\phi}{dt} = \Delta\omega + \frac{\omega_0}{Q_{ext}}\sqrt{\frac{P_i}{P_o}}\sin(\psi - \phi) \tag{2}$$

Here ϕ and ψ are the phases of the magnetron and injected signal, respectively. The same phenomenon of frequency locking occurs in semiconductors. Using this phenomenon, a combination of a magnetron and power source can be interpreted as a VCO (Voltage Controlled Oscillator), and phase adjustment and stabilization can be achieved by PLL (Phased Locked Loop) control. A system block diagram of the phase-controlled magnetron is shown in Fig. 2 [19]. We fabricated a phased array for microwave transmission using several such PCM units, and carried out successful experiments with beam control [19]. The experiments were performed with 2.45- and 5.8-GHz nonmodulated continuous wave (CW) operation. Very good phase stability (within 1°) was obtained, which is quite sufficient for phased arrays. In addition, a phase/amplitude-controlled magnetron with simultaneous control of both amplitude and phase was developed [20].

PCM offers phase control at low price and high efficiency, but even lower price and higher efficiency are required for the SPS. In PCM, a waveguide circulator is used for injection locking, which results in a 10% magnetron loss as well as additional weight. In addition, when a phased array is built, a phase shifter is required for every PCM unit. In this context, we propose a magnetron phased array with injection locking using microwaves leaked between the elements of the phased array (this method is sometimes adopted for semiconductor phased arrays).

4. Phase-Controlled Magnetron Phased Array Using Mutual Coupling

4.1 Basic theory

In semiconductor phased arrays, a semiconductor oscillator is locked by an injected signal using leak microwaves produced by mutual coupling between adjacent antennas, or microwaves coupled directly by lines or other means. This makes possible frequency stabilization and beam steering [21, 22]. The phases of semiconductor oscillators are determined following Adler's formula [21]:

$$\frac{d\phi_i}{dt} = \Delta\omega + \frac{\varepsilon_{i,j-1}\omega_i}{Q_{ext}}\sin(\phi_{i-1} - \phi_i) + \frac{\varepsilon_{i,j+1}\omega_i}{Q_{ext}}\sin(\phi_{i+1} - \phi_i) \quad (i = 1, 2, \cdots N) \tag{3}$$

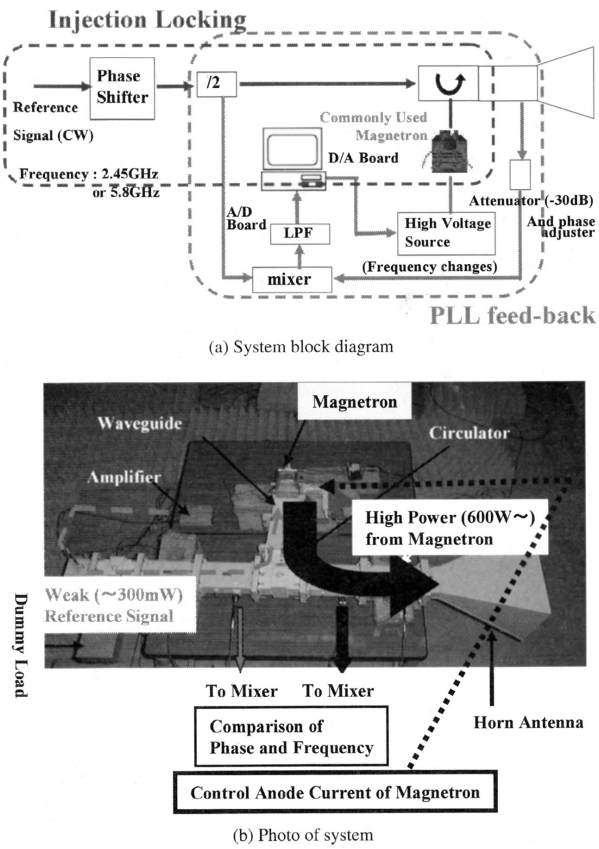

Fig. 2. Phased-controlled magnetron [19].

The above equation applies to the simultaneous equations that represent injection locking by mutual coupling between N oscillator elements; here ω_i and ϕ_i denote the self-excitation frequency and phase of the respective oscillators, and ε_{ij} is the coupling strength between the i-th and j-th elements. The coupling strength ε_{ij} between elements can be expressed as follows in terms of the power P_{ij} of the signal from the j-th oscillator to i-th oscillator, and the output power P_i of the i-th oscillator:

$$\varepsilon_{ij} = \sqrt{\frac{P_{ij}}{P_i}} \tag{4}$$

Since an oscillator has only one neighbor on each side, terms with the subscript 0 or $N + 1$ are ignored in Eq. (3). Assuming that all coupling strengths ε_{ij} are equal in Eq. (3), the self-excitation frequency of every oscillator can be set as follows so as to equalize the phase shifts on the ends:

$$\phi_i - \phi_{i-1} = \Delta\phi \ (\text{constant}) \tag{5}$$

Thus, the above expression is a solution to Eq. (3). Substituting Eq. (5) into Eq. (3) and assuming a steady state ($d\phi_i/dt = 0$), the following necessary condition for the self-excitation frequency of every oscillator can be derived:

$$\omega_i = \begin{cases} \omega_0 + \Delta\omega & (i = 1) \\ \omega_0 & (1 < i < N) \\ \omega_0 - \Delta\omega & (i = N) \end{cases} \tag{6}$$

Here ω_0 is the target output frequency, and $\Delta\omega = \varepsilon\omega_0/Q_{ext} \cdot \sin\Delta\phi$. That is, the phase shift between every oscillator and its neighbors on both sides can be made equal if the self-excitation frequency of both neighbors is changed by $\Delta\omega$ in opposite directions with respect to the target output frequency ω_0. Two values of $\Delta\phi$ exist for every $\Delta\omega$, but the phase shift $\Delta\phi$ between actual oscillators is restricted to the range of $-90° < \Delta\phi < +90°$. Therefore, $\Delta\phi$ is uniquely determined for every $\Delta\omega$, thus assuring beam steering. That is, beam control becomes possible without phase shifters if the oscillator frequencies are controlled as explained above. In a magnetron phased array, this means that beam steering by mutual coupling is possible provided that phase-controlled magnetrons are installed on both ends, and the rest are self-excitation magnetrons. This concept of a magnetron phased array is illustrated in Fig. 3.

4.2 Application to magnetron

However, the temperature dependence and other stability issues mentioned above will remain while the magnetron's self-oscillation is used unaltered. An example of the time variation of the self-oscillation frequency of a microwave cooker magnetron is given in Fig. 4.

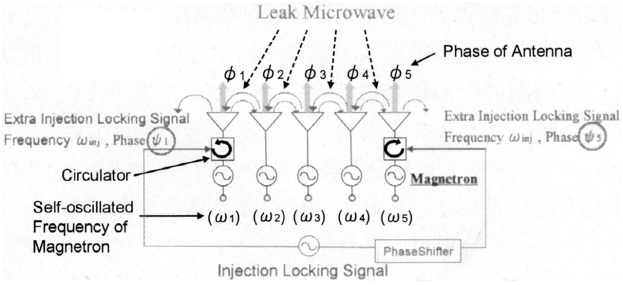

Fig. 3. Concept of phased arrays of PCM with mutual injection locking.

The variation amplitude is only about 6×10^{-5}, but experiments are required in order to determine whether mutual injection locking occurs at this magnitude of variation. In addition, magnetrons with the number $i = 1, N$ in Fig. 3 are subject to direct injection locking in Eq. (2), and therefore basic equation (3) must be combined with Eq. (2) in the case of a magnetron phased array with mutual injection locking:

$$\frac{d\phi}{dt} = \Delta\omega + \frac{\omega_i\rho_i}{Q_{ext}}\sin(\psi_i - \phi_i) + \frac{\varepsilon_{i,j-1}\omega_i}{Q_{ext}}\sin(\phi_{i-1} - \phi_i) + \frac{\varepsilon_{i,j+1}\omega_i}{Q_{ext}}\sin(\phi_{i+1} - \phi_i) \quad (i = 1, 2, \cdots N) \tag{7}$$

Here ρ_i is the amplitude of the external injection signal with respect to the amplitude of the microwaves emitted by the end magnetrons. The following can be obtained, with the microwave output power denoted by P_i and the power of the external signal denoted by $P_{inj,i}$:

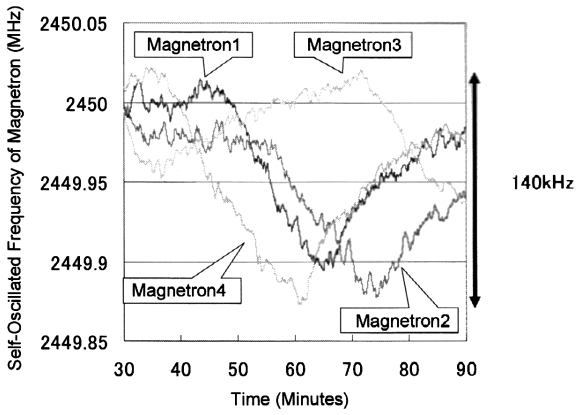

Fig. 4. Time variation of self-oscillation frequency of cooker-type magnetron.

$$\rho_{ij} = \sqrt{\frac{P_{inj,i}}{P_i}} \quad (i = 1, N) \tag{8}$$

Here ψ_i is the phase of the external injection signals on both ends. Both r_i and ψ_i exist only at $i = 1, N$; otherwise, they have zero values.

Suppose that all coupling strengths ε_{ij} and injection signal strengths ρ_i are equal in Eq. (7). Similarly to the previous section, by substituting Eq. (7) into Eq. (5) and assuming a steady state ($d\phi_i/dt = 0$), the following condition for the self-excitation frequency of magnetrons can be derived, under which the phase shift is divided equally among all antennas:

$$\omega_i = \begin{cases} \omega_{\text{int}} + \Delta\omega_1 & (i = 1) \\ \omega_{\text{int}} & (1 < i < N) \\ \omega_{\text{int}} - \Delta\omega_N & (i = N) \end{cases} \tag{9}$$

Here

$$\Delta\omega_i = \frac{\varepsilon\omega_i}{Q_{ext}} [\sin\Delta\phi - \sin(\phi_i - \psi_i)] \quad (i = 1, N) \tag{10}$$

Two values of $\Delta\phi$ exist for some $\Delta\omega_i$, but the phase shift $\Delta\phi$ between actual antennas is restricted to the range of $-90° < \Delta\phi < +90°$. In addition, suppose that the self-oscillation frequency of every magnetron coincides with that of the external injection signal, that is,

$$\omega_i = \omega_{inj} \quad \text{for all } i \tag{11}$$

In this case, $\phi_1 - \psi_1 = \Delta\phi$ and $\phi_N - \psi_N = \Delta\phi$ and therefore,

$$\psi_N - \psi_1 = (N + 1)\Delta\phi \tag{12}$$

That is, the phase shift between external injection signals can be distributed equally among all antennas if the self-oscillation frequency of every magnetron coincides with that of the external signal injected on both ends. If $|\psi_N - \psi_1| < 180°$, then $\Delta\phi$ is found uniquely. The case of $|\psi_N - \psi_1| > 180°$ is considered in the next section. In this system, too, one can easily imagine that instability of the magnetron's self-oscillation frequency may affect the stability of beam control. However, in contrast to the system explained in the previous section, the output frequencies stay synchronized to the injection signal frequency even though the self-oscillation frequency fluctuates, if the fluctuation is within the frequency lockable range.

4.3 Simulations

We conducted a number of simple simulations to investigate the basic properties of the system modeled by Eq. (7). In all the simulations mentioned in this section, unless otherwise noted, the number of antennas is $N = 4$, the magnetron's external Q-value is $Q_{ext} = 174$, and the phase difference between the external signals injected on the ends is $\psi_4 - \psi_1 = 90°$. Four antennas is a very small number compared to the several billion elements used in the SPS; however, this small number dictated by experimental limitations was considered sufficient for a basic understanding of external injection locking. The external Q-value was determined experimentally. First we examined the ideal state, assuming that the mutual couplings between adjacent antennas are of equal strength ε_{ij}, and that the external injection signals have the same power ρ. In this case, the phase shift between the external injection signals was divided equally provided that the self-excitation frequency ω_i of every magnetron coincided with the frequency ω_{inj} of the injected signal. The transient response for $\varepsilon = r = \sqrt{1\text{W}/500\text{W}} = 0.0447$ and $\omega_i = \omega_{inj} = 2.45$ GHz is shown in Fig. 5 (this response can be easily derived analytically as well). As is evident from the diagram, the system settles to a steady state in about 4 μs, and the phase is equally distributed.

Now consider a simulation allowing for scatter in the self-excitation frequencies of the magnetrons. The simulation was carried out using the frequency fluctuation data shown in Fig. 4 as well as actual data on magnetron radiated power. The other parameters were the same as in the previous simulation ($Q_{ext} = 174$, $\omega_{inj} = 2.45$ GHz, $P_{inj} = 1$ W). In addition, the power of the microwaves leaked between adjacent antennas was set to –30 dB with respect to the radiated power.

Figures 6 and 7 present simulation results obtained using a 1-hour portion of the measured data in Fig. 4 assuming that the phase difference between signals injected on the ends is $\psi_N - \psi_1 = 90°$. In particular, Fig. 6 shows the time variation of phase of every magnetron. Figure 7 shows a superposition of the beam patterns calculated for all

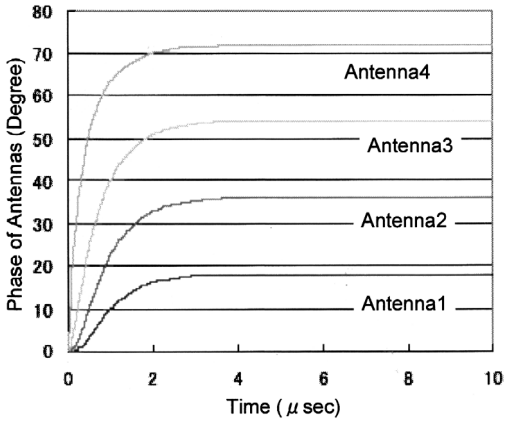

Fig. 5. Transient response under ideal conditions.

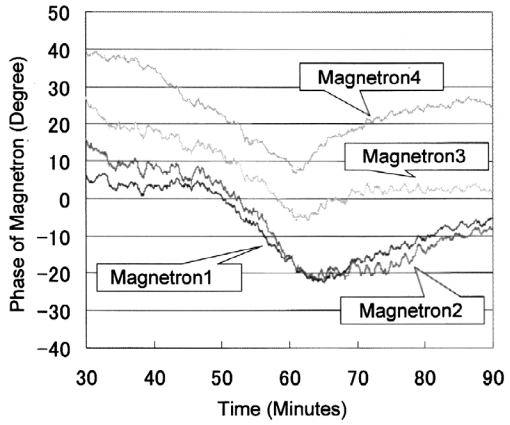

Fig. 6. Time dependence of phase of magnetrons.

1-minute portions of the data in Fig. 6. As is evident from Fig. 6, the phase of the magnetron outputs fluctuates strongly with the self-oscillation frequencies. However, these fluctuations correlate in phase with the respective antennas. Figure 7 indicates that the direction of the main beam does not change with time, and that the side lobes too remain almost unchanged. Thus, the proposed system allows beam steering of a phased array even though oscillators with an unstable self-oscillation frequency, such as magnetron, are employed.

4.4 Experiments

For verification of the above simulations, we conducted experiments with an actual magnetron phase array using mutual injection locking. The experiments were carried out on the same four magnetrons employed in the

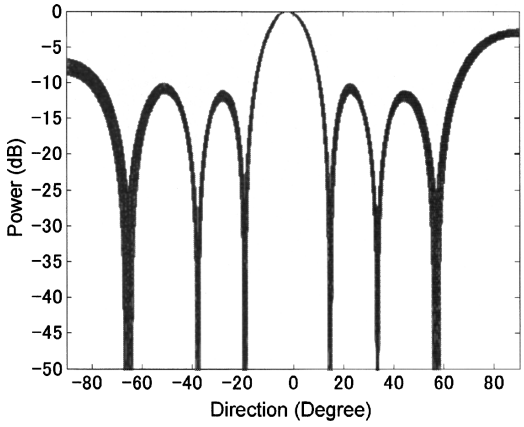

Fig. 7. Time dependence of beam pattern (only array factor).

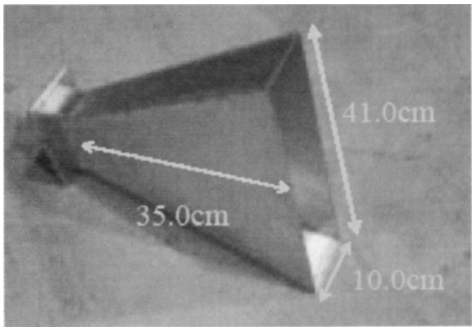

Fig. 8. Horn antenna used in experiments.

simulations (Fig. 4) using the horn antenna shown in Fig. 8. The one-dimensional array (see Fig. 9) was arranged with a pitch of about 10.5 cm (corresponding to the physical limit of 0.86 λ in the case of four elements), at a frequency of 2.45 GHz.

The configuration and appearance of the experimental system are shown in Figs. 10 and 11, respectively. Phase-controlled magnetrons were connected to both ends of the 1D four-element horn antenna array shown in Fig. 9, and self-excited magnetrons were used inside. The whole system was placed on a turntable in an anechoic chamber, and the beam patterns were measured.

The measured data for coupling between the array elements are given in Table 1. The coupling coefficients can be calculated from Eq. (2) using the data in the top row (marked). In order to compare actual and theoretical values, the parameters, including those required in Eq. (7), were measured as shown in Table 2.

Figure 12 shows the front-beam pattern of the phased array, which offers good agreement with the simulations

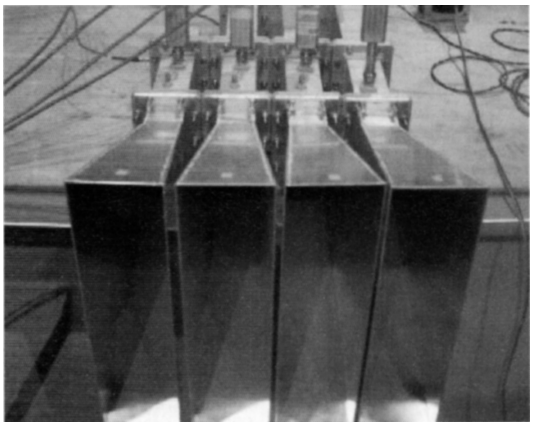

Fig. 9. 1D array used in experiments.

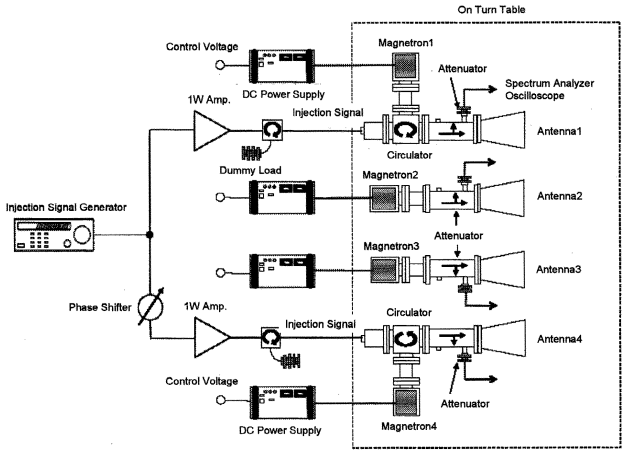

Fig. 10. Experimental setup.

(beam pattern synthesized from actual patterns of four horn antennas).

In addition, Figs. 13 to 15 show measured results of beam control for phase differences of 30°, 90°, and 150° between the end antennas and compare them with theoretical beam patterns calculated using the parameters in Table 2 and the simulation results obtained with Eq. (7). In addition, the measured and theoretical directions of the main beam at other values of the phase difference are given in Table 3. Thus, the measured results agree relatively well with the respective theoretical values at small phase differences; however, as the difference is increased, the discrepancies also grow. A detailed examination of the phase shifts at all antennas showed that although the distribution of the phase shift between all antennas is theoretically equal, in fact the phase shift increases toward the two inner antennas.

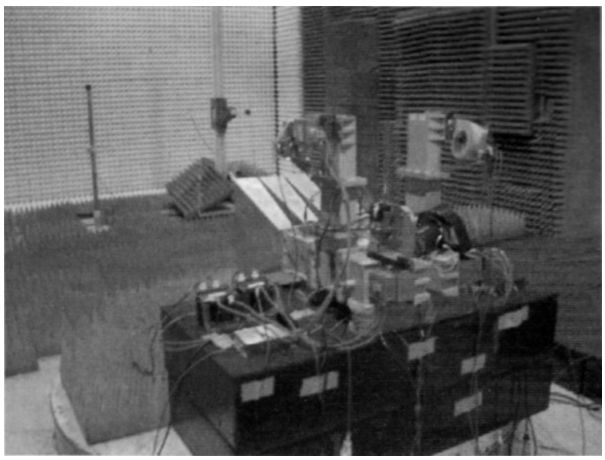

Fig. 11. Experimental system.

Table 1. Measured data of leak microwave power

	Leak Power (mW)	Leak Power／Radiated Power (dB)
From 1 Next ※	300	-33
From 2 Next	120	-37
From 3 Next	34	-44
From 4 Next	41	-43
From 5 Next	2	-56

Table 2. Parameters of experimental magnetron phased array

Frequency of External Injection Locking Signal	2.45GHz
Frequency of Self-Oscillated Frequency	2.45 for all i
Power of External Injection Locking Signal	1W
Radiated Power from Magnetron (i=1)	590W
Radiated Power from Magnetron (i=2)	490W
Radiated Power from Magnetron (i=3)	405W
Radiated Power from Magnetron (i=4)	440W
Ratio between Leak Power / Radiated Power	-33dB
External Q of Magnetron	174

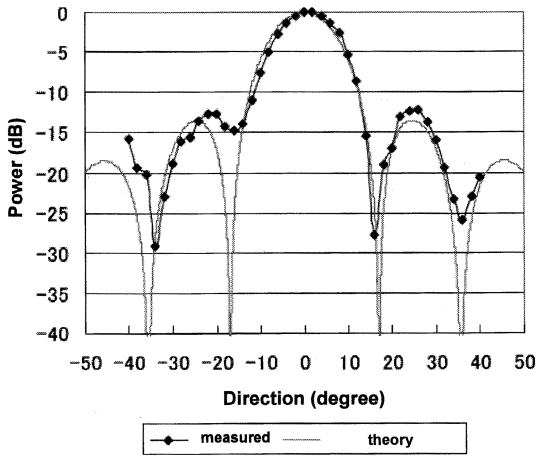

Fig. 12. Beam pattern (0°, front).

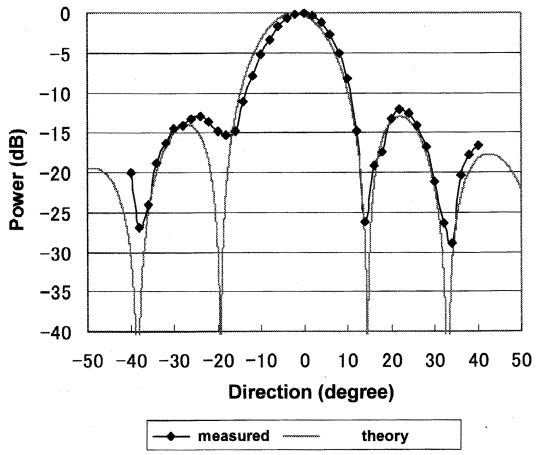

Fig. 13. Beam pattern (30° phase difference between edge antennas).

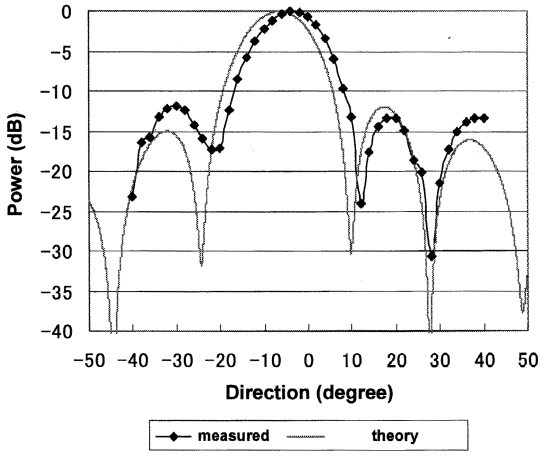

Fig. 14. Beam pattern (90° phase difference between edge antennas).

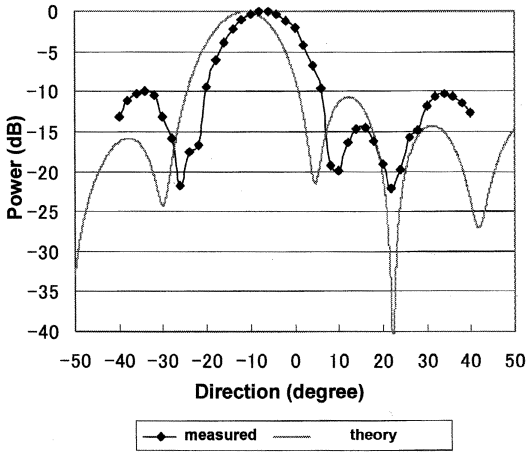

Fig. 15. Beam pattern (150° phase difference between edge antennas).

Table 3. Direction of main beam (measured and theoretical)

Phase Difference of Edge Antennas (°)	Direction of Main Beam (Measured) (°)	Direction of Main Beam (Theory) (°)	Error (°)
-150	+8	+11.2	-3.2
-120	+6	+8.75	-2.75
-90	+6	+6.46	-0.46
-60	+4	+4.26	-0.26
-30	+2	+2.13	-0.13
0	+2	0	-2
+30	0	-2.13	+2.13
+60	-2	-4.26	+2.26
+90	-4	-6.46	+2.46
+120	-6	-8.75	+2.75
+150	-6	-11.2	+5.2

The discrepancies between the theoretical phase values obtained by Eq. (7) and the experimental data are illustrated in Fig. 16.

4.5 Improved theory and experiments

The reason for the growing discrepancies between experimental and theoretical values at larger phase differences on the array ends appears to be that the leak power shown in Table 1 was larger than estimated, and that injection locking worked at this power. Equation (7) applies only to injection locking caused by leak power between neighbor elements; thus, we introduced another formulation that involves two more neighbors:

$$\frac{d\phi}{dt} = \Delta\omega + \frac{\omega_i \rho_i}{Q_{ext}} \sin(\psi_i - \phi_i) + \frac{\varepsilon_{i,j-1}\omega_i}{Q_{ext}} \sin(\phi_{i-1} - \phi_i) + \frac{\varepsilon_{i,j+1}\omega_i}{Q_{ext}} \sin(\phi_{i+1} - \phi_i) + \frac{\varepsilon_{i,j-2}\omega_i}{Q_{ext}} \sin(\phi_{i-2} - \phi_i) + \frac{\varepsilon_{i,j+2}\omega_i}{Q_{ext}} \sin(\phi_{i+2} - \phi_i) \quad (i = 1, 2, \cdots N) \tag{13}$$

We then repeated the simulations using Eq. (13). We used the results of calculations assuming the coupling strength ε between antennas in Table 2, and assuming leakage of –33 dB between neighbor elements and –37 dB between second neighbor elements. The resulting simulation results for the phase at every antenna with respect to the target phase difference between the array ends are shown in Fig. 17. As expected, an equal distribution of phase difference between antennas is not obtained when coupling between second

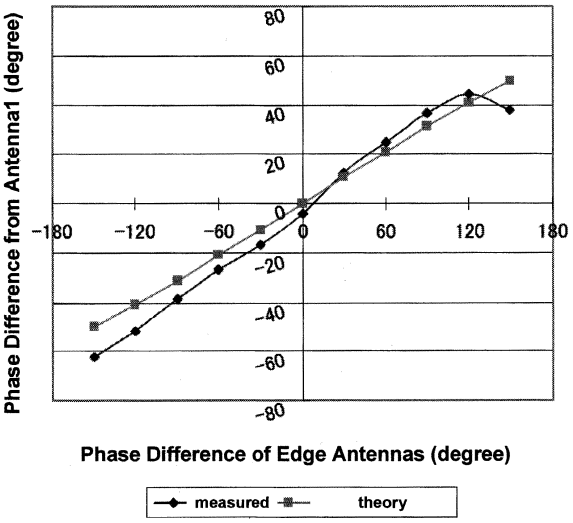

(a) Antenna 2

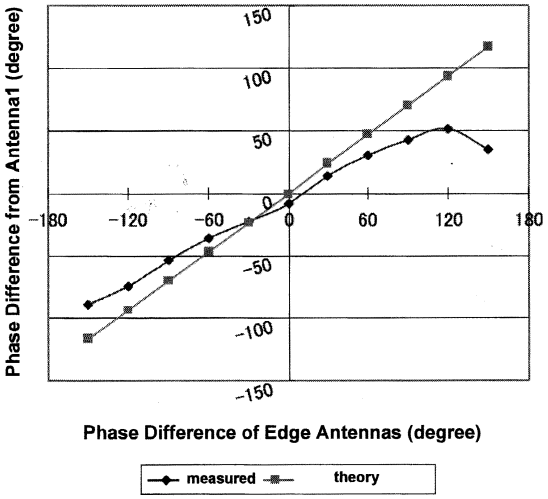

(b) Antenna 3

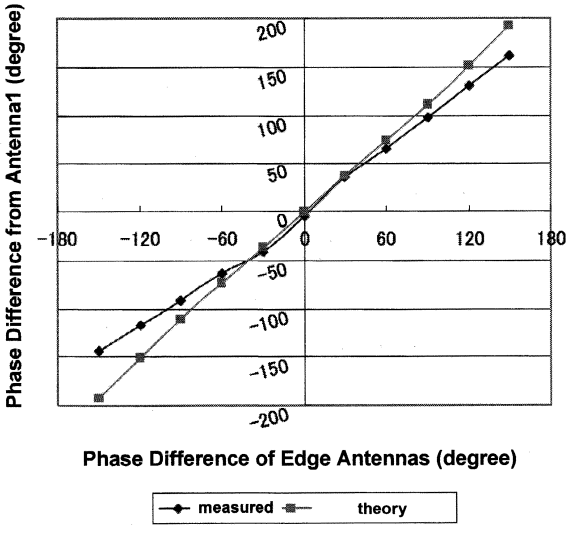

(c) Antenna 4

Fig. 16. Phase difference of antennas with respect to edge antenna (Antenna 1) (measured and theoretical).

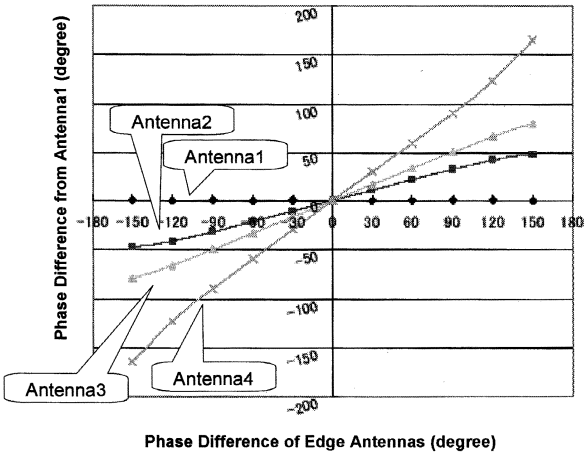

Fig. 17. Simulation results for phase difference of each antenna [by Eq. (13)].

neighbors is taken into account. In addition, the measured and simulated results for antenna phase with respect to Antenna 1 are shown in Fig. 18. Compared to Fig. 16, better agreement is achieved between the measured data and the simulations.

The measured beam direction values and the theoretical values recalculated using Eq. (13) are given in Table 4, and an example of a beam pattern at a phase difference of 90° between the end antennas is shown in Fig. 19. As is evident from these results, Eq. (13) gives more realistic theoretical values than Eq. (7).

Table 4. Direction of main beam [measured and theoretical by Eq. (13)]

Phase Difference of Edge Antennas (°)	Direction of Main Beam (Measured) (°)	Direction of Main Beam (Theory by Equation(13)) (°)	Error (°)
-150	+8	+9.12	-1.12
-120	+6	+6.81	-0.81
-90	+6	+4.99	-1.01
-60	+4	+3.27	-0.73
-30	+2	+1.63	-0.37
0	+2	0	-2
+30	0	-1.63	+1.63
+60	-2	-3.27	+1.27
+90	-4	-4.99	+0.99
+120	-6	-6.81	+0.81
+150	-6	-9.12	+3.12

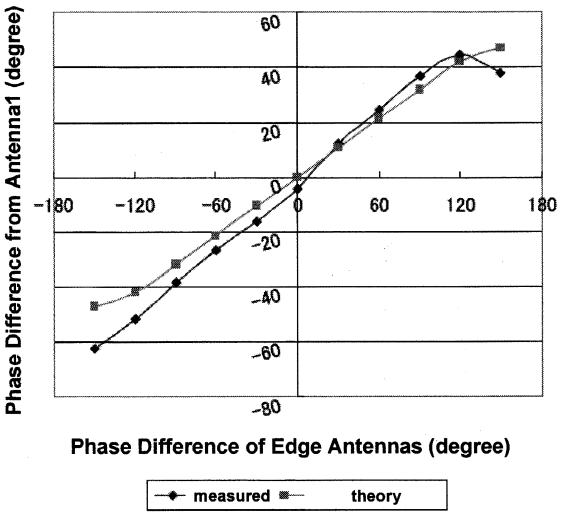

(a) Antenna 2

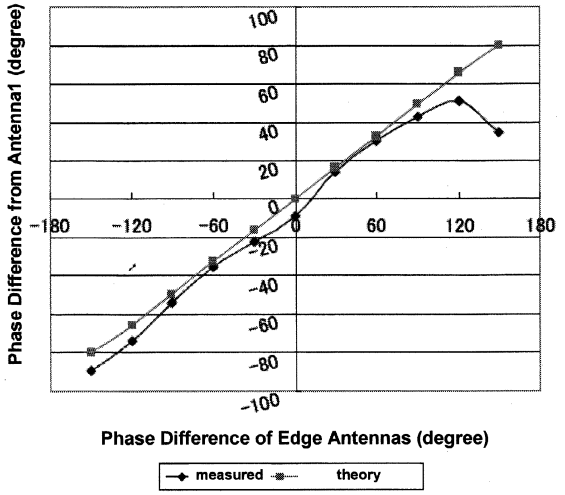

(b) Antenna 3

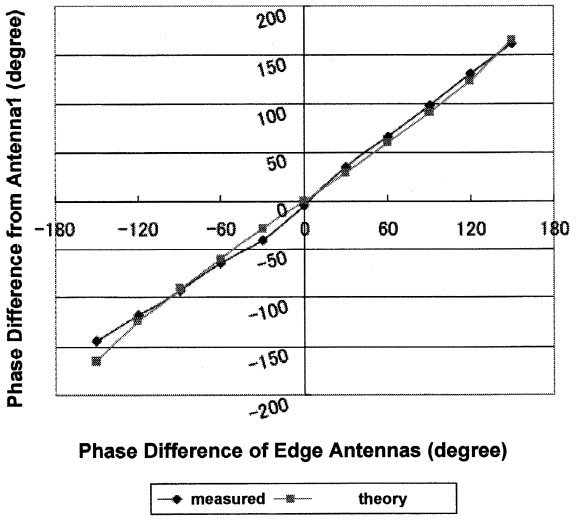

(c) Antenna 4

Fig. 18. Phase difference of antennas with respect to edge antenna (Antenna 1) [measured and theoretical by Eq. (13)].

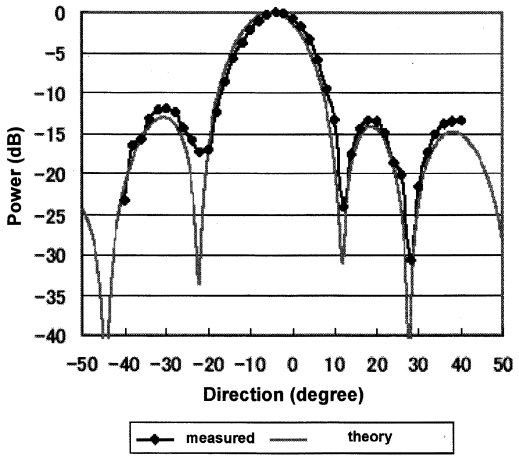

Fig. 19. Beam pattern (90° phase difference between edge antennas) [theoretical by Eq. (13)].

5. Conclusions

We have presented the results of applying mutual-coupling injection locking, which has hitherto been used only in semiconductor oscillator arrays, to a magnetron phased array. We have proposed a less expensive configuration of a phased array, with phase-controlled magnetrons used only on the ends, and have implemented beam steering. In addition, we have extended Adler's theoretical expression to phase-controlled magnetron arrays, and have proposed an improved theory with regard to leaks from second neighbors that offers more realistic calculated results. The theoretical discussions and experimental results presented in this study are only very basic results with respect to systems including billions of elements, as in the SPS. Nevertheless, the notion of controlling the self-oscillation of inner elements by end phase shifters can be used for SPS in terms of oscillation control by interaction between the phase shifters provided individually for multiple elements. As a matter of fact, we may expect more complex interaction and behavior in this case, which requires further improvement of Eq. (13) and additional investigation by simulations and experiments.

Acknowledgments

This study was performed with cooperation by H. Mizutani, then a postgraduate student at Kyoto University. In addition, the experiments were conducted using the METLAB microwave energy transmission system at the Research Institute for Sustainable Humanosphere, Kyoto University.

REFERENCES

1. Yoshioka K et al. CO_2 load of space solar satellites. Project for the Future WG2-1, 19, 1998.
2. Brown WC. The history of power transmission by radio waves. IEEE Trans MTT 1984;32:1230–1242.
3. Glaser PE. Power from the sun: Its future. Science 1968;162:857–886.
4. DOE and NASA Report. Satellite power system: concept development and evaluation program. Reference System Report, 1979.
5. Matsumoto H. Research on solar power station and microwave power transmission in Japan: Review and perspectives. IEEE Microwave Magazine, No. 12, p 36–45, 2002.
6. Fujita M et al. Present state of research in space energy systems (SSPS) at JAXA. Tech Rep IEICE 2007;SPS2007-01:7–10.
7. Mihara S et al. USEF activities in SSPS. Tech Rep IEICE 2007;SPS2007-01:1–6.
8. Mankins JC. A fresh look at the concept of space solar power. Proc of 3rd Int Conf on Solar Power from Space—SPS'97, S7041.
9. Summerer L, Ongaro F. Solar power from space—Validation of options for Europe. Proc of 4th Int Conf on Solar Power from Space—SPS'04, p 17–26.
10. Meadows DH, Meadows DL, Randers J, Behrens WW III. The limits to growth—A report for THE CLUB OF ROME'S project on the predicament of mankind. Universe Books; 1972.
11. Yamagiwa Y, Nagatomo M. An evaluation model of solar power satellites using world dynamics simulation. Space Power 1992;11:121–131.
12. Mitsubishi Research Institute Report. Complex research in space energy systems, 2005.
13. Brookner E. Phase arrays and radars—Past, present and future. Microwave Journal, Cover Feature, No. 1, 2006.
14. ISCS Trans on Satellite Communications, No. 71, p 19–43.
15. Mitani T, Shinohara N, Matsumoto H, Hashimoto K. Improvement of spurious noises generated from magnetrons driven by DC power supply after turning off filament current. IEICE Trans Electron 2003;E86-C:1556–1563.
16. Mitani T et al. Temporal analysis of noise generated by microwave cooker magnetrons. IEICE Trans 2004;J87-C:1146–1154.
17. Shinohara N et al. R&D in phase-controlled magnetrons. IEICE Trans 2001;J84-C:199–206.
18. Adler R. A study of locking phenomena in oscillators. Proc of I.R.E. and Waves and Electrons 1946;34:351–357.
19. Shinohara N, Matsumoto H, Hashimoto K. Phase-controlled magnetron development for SPORTS: Space power radio transmission system. The Radio Science Bulletin, No. 310, p 29–35, 2004.
20. Shinohara N, Matsumoto H. Phase array technology with phase and amplitude controlled magnetron for microwave power transmission. Proc of 4th Int Conf on Solar Power from Space—SPS'04, p 117–124.
21. York RA, Itoh T. Injection- and phase-locking techniques for beam control. IEEE Trans MTT 1998;46:1920–1929.
22. Stephan KD, Morgan WA. Analysis of interinjection-locked oscillators for integrated phased arrays. IEEE Trans AP 1987;35:771–781.

AUTHORS

Naoki Shinohara (member) received a bachelor's degree from Kyoto University in 1991, completed the M.E. and doctoral programs in 1993 and 1996, and joined the Radio Atmospheric Science Center of Kyoto University as a research associate. He became a research associate at the Radio Science Center for Space and Atmosphere in 2000, an associate professor in 2001, and an associate professor at the Research Institute for Sustainable Humanosphere in 2004. His research interests are SPS and microwave energy transmission. He holds a D.Eng. degree, and is a member of IEEE, URSI, and IEICE.

Hiroshi Matsumoto (nonmember) received a bachelor's degree from Kyoto University in 1965, and completed the M.E. program in 1967. He was appointed a professor at the Radio Atmospheric Science Center of Kyoto University in 1977, head of the Center from 1992 to 1998, professor at the Radio Science Center for Space and Atmosphere in 2000, director of the Center in 2002, professor at the Research Institute for Sustainable Humanosphere and Director of the same institution in 2004, Vice President of Kyoto University in 2005, and since 2008 President of Kyoto University. He is professor emeritus at Kyoto University and a visiting professor at ISAS and Wuhan University (China). His research interests are space plasma physics, space radio engineering, and space energy transmission. He received the Tanakadate Award in 1975, NASA Group Achievement Award in 1993 and 1998, AGU (JGR) Fellow in 1998, Shida-Rinzaburo Award in 1999, IEEE Fellow in 2002, RAS-Associate Award (UK) in 2004, Russian Federation of Cosmonautics Gagarin Medal in 2006, and Minister of MEXT Award in 2006. He is an SGEPSS Council member, and former chairman, and URSI former chairman. He is a member of AGU.